CHAPTER 7
STRAIN MODELING

In this chapter, the amount of shear that has been accommodated by the SC-like LOFZ system introduced in the previous chapters will be quantified using a simple kinematic model. The underlying concept of the kinematic model is that the major strike-slip faults correspond to the directions of maximum angular shear strain within a hypothetical 2-D (horizontal) strain ellipse which is the result of bulk homogenous simple shear.

7.1 Theoretical background

A strain ellipse generally contains two lines a and b on which angular (tangential) shear strains ψ are maximal (i.e., the directions of maximum angular shear strain) but of opposite senses (Fig. 7.1). These lines define an angle φ with the long axis of the strain ellipse (e_1) which is 45° in the undeformed state (Fig. 7.1 a) and decreases during progressive deformation according to Wettstein´s equation

$$\varphi = \arctan (1/R) \qquad \text{(E 7.1)}$$

where R is the ellipticity of the finite strain ellipse (Wettstein, 1886).

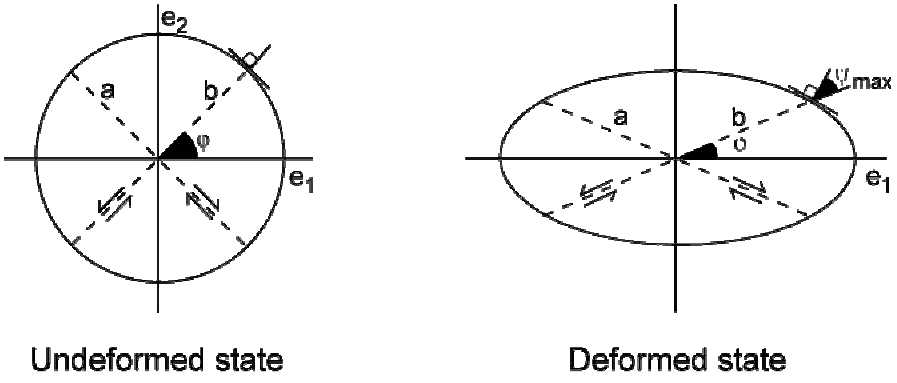

Fig. 7.1: *Relation between the directions of maximum tangential shear strain and the strain ellipse.*

The orientation of the lines a and b thus defines both the shape (ellipticity) and the orientation of the (finite) strain ellipse. The shear strain γ necessary to produce the finite strain ellipse is then given by

$$\gamma = \tan \psi = (R^2-1) \tan\varphi / (1+R^2\tan^2\varphi) \qquad \text{(E 7.2)}$$

(e.g. Ramsey and Huber, 1983). The orientation of the shear plane with respect to the strain ellipse is given by

$$\tan 2\theta = 2/\gamma \qquad \text{(E 7.3)}$$

where θ is the angle between the long axis of the finite strain ellipse (e_1) and the shear plane (e.g. Ramsay and Graham, 1970).

7.2 Kinematic model

The above equations have been applied to the fracture system observed in the study area based on the following assumptions:

- Faults observed in the study area define a kinematically coupled fault system with SC-like shear zone geometry composed of arc-parallel dextral strike-slip faults and arc-oblique sinistral strike-slip faults (Fig. 7.2). This simplification does not account for oblique slips on faults and implies plane strain conditions, i.e. no vertical thickening or thinning of the shear zone. Although several arc-parallel faults show indications of normal faulting in the field suggesting transtension, the rather normal crustal thickness of the crust in the Southern Andes (ca. 35 - 40 km, Bohm et al., 2002) indicate that at crustal scale deformation does not include components of significant thickening or thinning.

- The observed fault pattern reflects strain localization and strain partitioning within a shear zone that undergoes bulk homogeneous deformation, i.e. heterogeneous strain at regional scale reflects crustal scale homogeneous strain.

- The state of stress within the shear zone is favorable for reactivation of pre-existing faults. It is likely that fluid pressures within the crust (either induced by melt or hydrous fluids) are close to lithostatic pressures within the intra-arc region. If, under such conditions, differential stresses are low, pre-existing faults can be reactivated even in cases where the angle between the maximum stress and the fault plane is 45 - 90° (Secor, 1965, Etheridge, 1983, see also Ch. 5.5.3).

- Shear is taken up entirely within the shear zone; there is no horizontal slip along the shear zone boundaries. The viability of this assumption is verified by the lack of major arc-parallel strike-slip faults at the margins or the intra-arc zone.

Fig. 7.2 shows the inferred finite strain ellipse of the study area. Major strike-slip faults trend ca. N10°E (dextral) and ca. N40°W (sinistral). Consequently, the angle 2φ between the two directions of maximum angular shear strain is about 50°. From equation E 7.1 follows that the finite strain ellipse has an ellipticity R = 2.14 indicating 47% stretching parallel to its long axis e_1 (oriented N15°W, i.e. the half angle between the major strike slip faults) and 32% shortening parallel to its short axis e_2 (oriented N75°E). According to equation E 7.2, the imposed shear strain γ is 0.84 and the angular shear strain ψ is 40°. Since e_1 is oriented N15°W and the shear strain γ is 0.84, equation E 7.3 yields that the orientation of the shear plane in the study area is N19°E which is consistent with the trend of volcanic arc (N10-20°E). Knowing the shear strain, the amount of total displacement across the shear zone can be calculated from the width of the shear zone. The LOFZ is an 80 – 150 km wide fault zone system (Ch. 5.5). Assuming a mean shear zone width of 100 km, 84 km of dextral displacement has been accommodated by the shear zone.

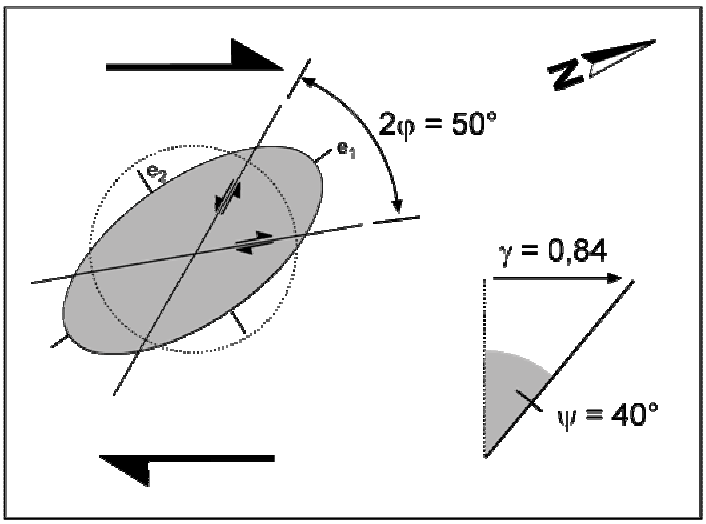

Fig. 7.2: *Hypothetical finite horizontal sectional strain ellipse of the study area.*

7.3 Sensitivity analysis

A sensitivity analysis has been performed to determine how variations of critical model parameters affect the estimate of the total displacement across the shear zone. Two

parameters the displacement estimate: the angle 2φ between the major sinistral and dextral faults and the shear zone width (W).

Variation of 2φ

The model calculations are based on an angle 2φ of 50° which has been inferred from lineament and drainage network analysis. 2.5° is assumed as a reasonable variation of the lineament orientations reflecting method internal errors resulting from distortion inherent in the satellite image and digitalization errors and natural scatter. Since this variation affects both the orientation of arc-parallel and arc-oblique faults, the resulting variation in angle 2φ may be as large as 10° (45 - 55°). Consequently, for a shear zone width of 100 km, the estimated range of displacement across the shear zone may vary between 70 and 100 km.

Variation of W

Variation of the width of the shear zone W may also impose a variation of the displacement estimates. In the model, a mean shear zone width of 100 km has been assumed which corresponds to mean width of the actual volcanic arc. The minimum width of the volcanic arc is about 80 km. Since the boundaries of the shear zone are not well defined, however, the shear zone may be as wide as 150 km which is the maximum E-W distance between the eastern border of the longitudinal valley (defined as the transition between Quaternary infill of the valley and basement outcrops of the main cordillera) and the easternmost faults which may be interpreted as part of the shear zone (Fig. 5.19). For a 2φ-angle of 50°, the minimum and maximum displacements are consequently 67 km and 126 km, respectively.

Maximum and minimum displacement

Maximum and minimum displacement estimates has been calculated by combining the highest and lowest values of 2φ and W, respectively, for a minimum estimate and the lowest and highest values of 2φ and W, respectively, for a maximum estimate. Accordingly, the highest and lowest displacements are 56 and 150 km, respectively. This is consistent with the field observations and the model assumptions.

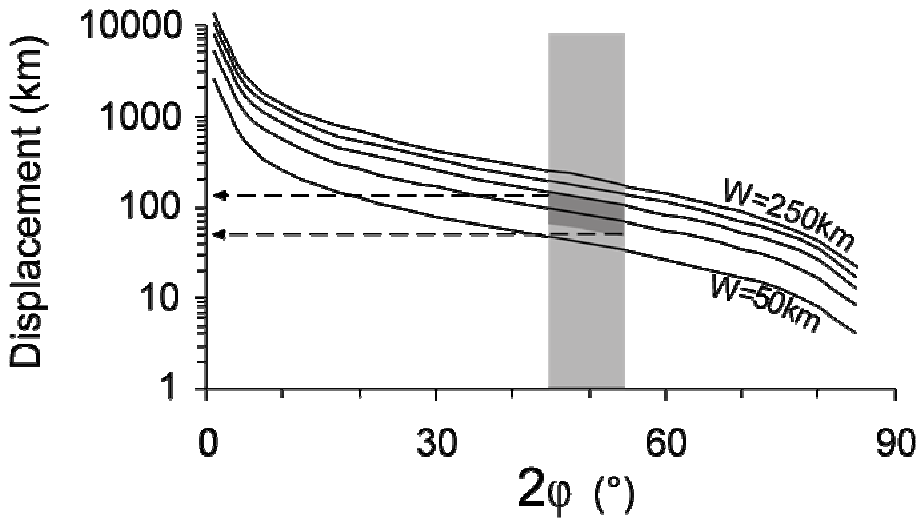

Fig. 7.3: *Sensitivity analysis. Error sensitivities for total displacement across the shear zone varying the angle 2φ between major strike-slip faults and shear zone width (W, contours from 50 to 250 km with 50 km contour intervals). The gray bar indicates the range of 2φ angles observed in the study area (45 - 55°). For a shear zone width of 80 – 150 km, the solution space (dark gray area) indicates displacements between 56 and 150 km.*

7.4 Other kinematic constraints

7.4.1 Rotations

The pattern of vertical axis block rotations in the Southern Andes involves both clockwise and anti-clockwise rotations: Garciá et al. (1988) reported vertical axis rotations of paleomagnetic poles within the Main Cordillera between 39° and 40°S. Their dataset shows a bimodal distribution with ca. 45° dextral rotations in the vicinity of the main trace of the LOFZ and almost no or slightly counter-clockwise rotations distant from the LOFZ trace which they interpreted as an indication for small crustal blocks moving independently in a distributed shear zone. Rotations affected rocks as young as 3 – 4 Ma indicating that the movements are recent. Between 42° and 43°S, Rojas et al. (1994) derived post-Miocene, counter-clockwise rotations of ca. 15° west of the LOFZ main trace which they interpreted as evidence for large-scale imbrication of crustal fore-arc blocks in the horizontal plane in response to oblique subduction ("buttressed sliver" model of Beck et al., 1993). At the same latitude east of the LOFZ main trace, dominantly clockwise rotations but also some anti-clockwise rotations are reported (Cembrano et al., 1992, Beck et al., 1998, 2000) suggesting distributed shear within a zone which extends from the main LOFZ trace at least 50 km to the east.

Apart from paleomagnetic techniques, block rotations can be identified by the rotation of passive markers. In the study area such possible passive markers are (a) map-scale thrusts and fold axis which formed prior to Pliocene, and (b) volcanic dykes. Throughout the study area, fold-axis developed during Late Miocene basin inversion trend N-S, parallel to cogenetic inverse faults (Fig. 4.4). Map-scale folds form undisrupted trails over tens of kilometers length suggesting that they have not been affected by rotation of km-scale blocks. Volcanic dykes in the study area also show a well defined bimodal distribution (NNE-SSW and SW-NE) consistent with crustal-scale extensional fractures indicated by elongate volcanoes (Fig. 3.10). This stable orientation of passive markers indicate that large areas have not been rotated significantly (probably less than 10°) during the Late Cenozoic. This argues clearly against large-scale block-rotation models. Large rotations (> 30°) observed locally along traces of faults suggests moreover that rotational deformation has been localized along major fault zones. Off these fault zones, large areas appear undeformed. The SC-geometry of the fault system led consequently to rhomb-like fault-bound domains within the intra-arc zone similar to the segmentation of the Central Andean Plateau proposed by Riller and Oncken (2003) or the partially rigid "soft dominos" by Walsh and Watterson (1991) and Peacock et al. (1998).

Local rotations along dextral and sinistral faults expected from the here presented model are composed of two components: (1) line rotation $\Delta\Theta$ and (2) rotation induced by tangential shear Ψ (Fig. 7.4 a). The line rotation is the difference in orientation of the directions of maximum tangential shear (i.e., the fault) in the undeformed and deformed state and is anticlockwise for dextral faults and clockwise for sinistral faults during dextral simple shear. Rotation induced by tangential shear ψ is clockwise for dextral faults and anticlockwise for sinistral faults. Figure 7.4 b shows the evolution of net rotations along dextral and sinistral faults during progressive deformation assuming a shear zone width of 100 km.

It is obvious from Fig. 7.4 that deformation results in a bimodal distribution of net rotations with small (< 10°) anti-clockwise net rotations along sinistral faults and large (> 30°) clockwise net rotations along dextral faults. This result is consistent with the existing paleomagnetic datasets: The dataset of Garciá et al. (1988) shows that sites in the vicinity of N-S oriented, dextral faults have been rotated clockwise up to 33° during the last 3 – 4 Ma. If this value is considered as rotation along dextral faults in our model, this suggests fore-arc displacement of about 90 km since the Pliocene consistent with the fault pattern based prediction of the kinematic model.

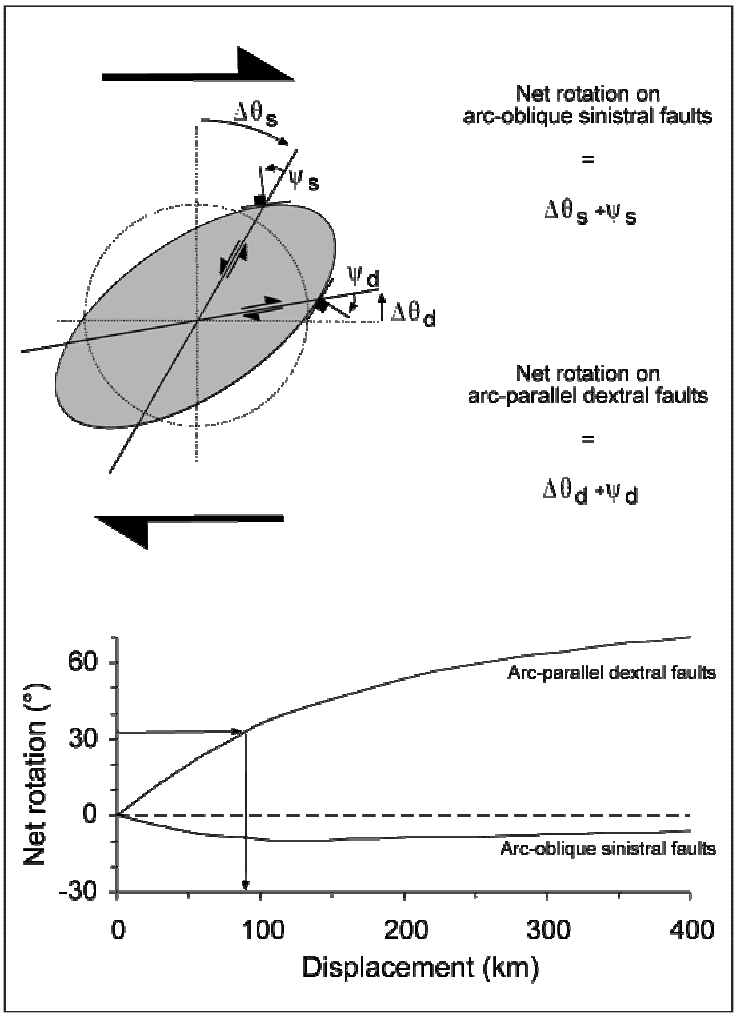

Fig. 7.4: *Rotation during simple shear (clockwise rotations positive).*

7.4.2 Translation and displacement

Finite strike-slip displacement across the LOFZ and translation of a fore-arc sliver (the Chiloé block) can be constrained using (1) paleomagnetic inclinations and (2) offset markers. Paleomagnetic studies demonstrated that rocks east of the LOFZ remained stable with respect to the South American craton (Cembrano et al., 1992, Butler et al., 1991, Beck et al., 1988) whereas rocks west of the LOFZ may have moved northward by 300 – 500 km since the Miocene (Rojas et al., 1994, Garciá et al., 1988). However, taking into account the large errors of these determinations (ca. 500 km), this constraint has to be considered with caution.

Offset markers which can be potentially used to constrain displacement across the LOFZ are rare. The Gastre Fault Zone (GFZ), a Late Paleozoic/Early Triassic (Rapela and Pankhurst, 1992, Glodny et al., 2002) shear zone crossing the South American continent in a northwesterly direction shows a dextral displacement across the LOFZ of

ca. 120 km (Rapela and Pankhurst, 1992, Fig. 7.5 a) which places an upper limit of total post-Triassic dextral displacement across the LOFZ.

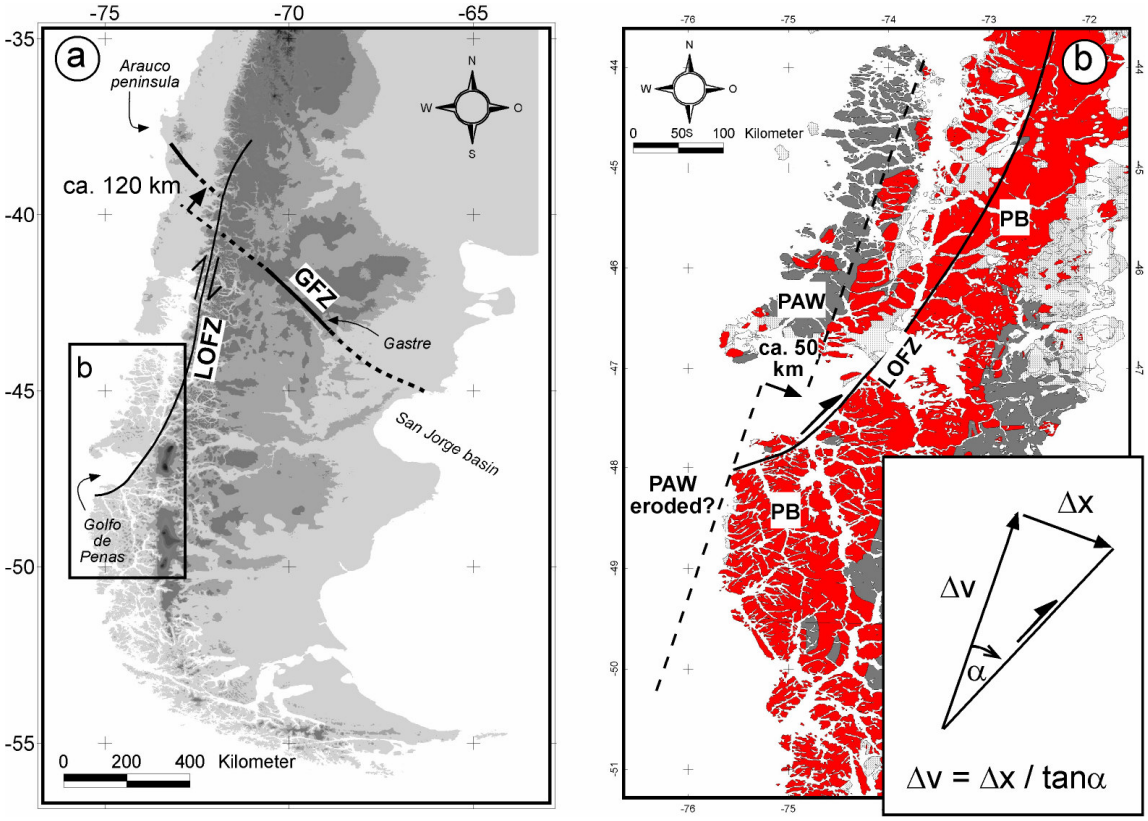

Fig. 7.5: *Offset constraints. Abbreviations: GFZ = Gastre fault zone, LOFZ = Liquiñe-Ofqui fault zone, PB = Patagonian Batholith, PAW = paleoaccretionary wedge.*

The Patagonian Batholith (PB) strikes parallel to the continental margin and shows an E-W displacement across the Golfo de Peñas where the LOFZ terminates (Fig. 7.5 b). North of the Golfo de Peñas, the PB froms the basement of the active volcanic arc and the fore-arc basement consists of a paleoaccretionary wedge (the Western Series, Hervé, 1977, Ch. 1.4.2), whereas to the south, the PB is situated wholly in the fore-arc position and the Western Series is absent (Hervé et al., 2000). Postulating that the paleoaccretionary wedge/Western Series south of the Golfo de Peñas has disappeared due to subduction erosion, a reconstruction yields that the PB has been displaced landwards across the LOFZ by at least 50 km (Δx in Fig. 7.5 b). 50 km landward displacement can be explained by ca. 60 – 86 km of margin-parallel, northward translation of the fore-arc north of the Golfo de Peñas (Δv in Fig. 7.5 b) along the southern terminus of the LOFZ which strikes here 30 – 40° (α in Fig. 7.5 b) oblique to the continental margin.

60 – 86 km margin-parallel displacement of the PB and 120 km dextral offset of the GFZ are minimum and maximum amounts, respectively, for the northward displacement of the Chiloé block and are consistent with the fault pattern based prediction of the kinematic model.

7.5 Timing of deformation

The LOFZ has been considered by previous workers as a long-lived structure, active at least since the Cretaceous (e.g. Cembrano et al., 1996, Hervé, 1994). However, this hypothesis is based on few lines of evidence and is far from being conclusive.

7.5.1 Ductile shear zones

Cembrano et al. (2000, 2002) gave the most comprehensive database evidencing ductile deformations predating brittle LOFZ tectonics in the study area. Most of these data indicate that LOFZ deformation was initiated during the Late Miocene. South of 42°S, where exhumation rates are high (Thomson, 2002), isotopic ages from ductily deformed granitoids and country rocks suggest Late-Miocene to Pliocene strike-slip activity within the intra-arc zone. At 42°S, mylonitic dextral strike-slip shear zones, developed from Late Miocene granitoids vary in age between 3 and 7 Ma (Ar-Ar/biotite) (Cembrano et al., 2000, see also Ch. 4.5 of this work). Between 44 and 46°S, mylonitic shear zones developed from Late Miocene granitoids indicate dextral transpression around 4 Ma (Cembrano et al., 2002).

Only at one locality in the study area, pre-Miocene ductile fabrics has been observed, namely at Liquiñe (40°S, see Ch. 4.4). There, a mylonitic foliation is developed from a migmatitic layering. Cembrano et al. (2000) dated a dike cross-cutting this foliation as 100 ± 2 Ma (Ar-Ar/hornblende) and interpreted the foliation as reminiscence of pre-Mid Cretaceous strike-slip deformation along the LOFZ. However, as discussed in the Ch. 4.4 of this work, ductile fabrics in the Liquiñe area most likely reflect deformation of the wall rock due to pluton emplacement. If this interpretation is valid, Cretaceous fabrics in the Liquiñe area cannot further be considered as a testimony for a Mesozoic LOFZ activity.

7.5.2 Pull-apart basins

The presence of Eocene – Miocene volcano-sedimentary, partly marine sequences along the LOFZ and in the fore-arc (Ayacara basin at ca. 42°S, Traiguen Basin at ca. 44°S) has been interpreted as pull-apart basins developed along the LOFZ thus indicating its Cenozoic activity (Hervé et al., 2000, Thomson, 2002). However, the structural evolution of theses basins has not been studied in detail yet.

Levi et al. (1966) were the first who described the Fm. Ayacara as a several hundreds of meters thick volcano-sedimentary sequence with indications for turbiditic mass flows. Microfossils indicate an Eocene – Miocene age (Martínez, 1961). Based on a correlation of several sections, Rojas et al. (1994) basically confirmed these earlier findings and interpreted these sequences as being deposited in marine basins, which may represent voids created by block rotations induced by oblique subduction. As they pointed out in their paper, this interpretation is highly speculative.

The Fm. Traiguén has been originally described by Hervé et al. (1995) as a marine volcano-sedimentary sequence including MORB-type pillow basalts. The age of the rocks is considered to be between 46 and 20 Ma based on two weak Rb-Sr whole rock errorchrons (20 ± 28 Ma Seno Soto slates, and 20 ± 26 Ma Isla Magdalena metabasalts) and microfossils (Hervé et al., 1995, and references therein). Hervé et al. (1995) interpreted these deposits as remnants of a marine basin associated with strike-slip tectonics along the LOFZ.

However, to the authors knowledge, there exist no detailed tectono-sedimentary studies of these basins which could verify the speculative models of Rojas et al. (1994) and Hervé et al. (1995) linking the basins structurally to the LOFZ. Instead, Jordan et al. (2001) showed that mid-Cenozoic basins occurred all along the active margin in the fore-arc as well as in the back-arc. They found no structural evidence for a pull-apart evolution of these basins and suggested in contrast, that they formed during a mid-Cenozoic phase of regional extension normal to the margin.

7.5.3 Evidences for Pliocene - active deformation

Several evidences support the hypothesis that the brittle strike-slip LOFZ is as young as Pliocene and is still active today:

- In the Lonquimay area (38°S) brittle faults of the LOFZ crosscut folds developed during the Late Miocene.

- Rocks as young as 3 – 4 Ma has been affected by large (~ 30°) vertical axes rotations which are associated to strike-slip LOFZ tectonics (Garciá et al., 1988).

- Late Pliocene caldera formation (2 - 2.6 Ma, Linares et al., 1999) is genetically linked to strike-slip faulting (Muñoz and Stern, 1988, Folguera and Ramos, 2000, Folguera et al, 2002).

- Numerous graben structures filled with Holocene fluvial deposits (e.g. the Lonquimay graben) along strike of the volcanic arc and the formation of a prominent escarpment at the southern termination of the LOFZ in the Golfo de Penas (Diemer and Forsythe, 2000) suggest that LOFZ-related tectonics has been active during the past few million years.

- Brittle strike-slip faulting affects Holocene terraces in the Reloncaví fjord (Thiele et al., 1986), Quaternary deposits in the San Rafael area (Wood, 1989), and Holocene lava flows of the Copahue (Melnick, 2000) and Apagado (Alarcón, 1995) volcanoes indicating Holocene activity of the LOFZ.

- Microseismicity has been detected at the southern end of the LOFZ indicating its activity (Murdie et al., 1993).

- Two focal plane solutions determined from earthquakes associated with the eruptions of the Lonquimay volcano in 1989 (Barrientos and Acevedo, 1992) and of the Hudson volcano in 1965 (Chinn and Isacks, 1983) indicate active dextral strike-slip motions along arc-parallel subvertical faults.

The present-day deformation of the study area as inferred from GPS-data is strongly affected by postseismic relaxation effects of the 1960 Valdivia earthquake (Klotz et al., 2001) and do not permit a reliable interpretation in terms of permanent (plastic) deformation. Apatite fission track data (Gräfe, pers. comm.) indicate that along E-W profiles across the cordillera no differential exhumation occurred since the Pliocene indicating exclusively strike-slip movements since. From the here presented evidences, it is suggested that the LOFZ has been active as an intra-arc strike slip fault system during the past 3 - 5 Ma.

7.6 Discussion

7.6.1 Consistency with plate kinematic parameters

Most authors agree that oblique subduction is the driving force for margin-parallel shear in the overriding plate (Fitch, 1972, Jarrard, 1986, McCaffrey, 1992, Cembrano et al. 2002). If this is true, strain rates of deformation in the overriding plate should be consistent with plate kinematic constraints. The here proposed kinematic model allows for the first time to evaluate the displacement rate along the LOFZ. The model suggests that 84 km (+66, -28) of margin-parallel dextral shear has been accommodated during the last 3 - 5 Ma. The resulting rate of margin parallel shear is then about 17 – 28 mm/a. How does this result fit to plate kinematic constraints?

Although obliquity increased during the Neogene, the resultant margin-parallel shear has not changed significantly, because convergence has coevally accelerated (Figs. 7.6 a, c). Averaged over the past 5 Ma, the Nazca and South American plates has converged with a mean velocity of 78 mm/a in a direction of N75°E with respect to stable South America (Fig. 7.6 a, Somoza, 1998). At 40°S, this is about 25° oblique to the continental margin which trends N10°E. Decomposition of the plate convergence vector yields 34 mm/a of a dextral shear component (Fig. 7.6 b) which has to be accommodated either at the plate interface by oblique thrusting or by deformation of the overriding plate. Focal plane solutions of thrust earthquakes in the fore-arc region of the Southern Andes (Asch et al., 2001, Reinecker et al., 2003, Harvard CMT) show that shortening accommodated in the accretionary wedge is oriented N80-90°E, indicating that thrusting has a significant component of obliquity today (~ 15°) with respect to the trench line normal (Fig. 7.6 d). Consequently, the shear component that is partitioned into the overriding plate is reduced to ~ 15 mm/a. This value is consistent with the lower limit of displacement rates predicted by the here presented model (17 mm/a) and demonstrate its consistency with plate kinematic parameters.

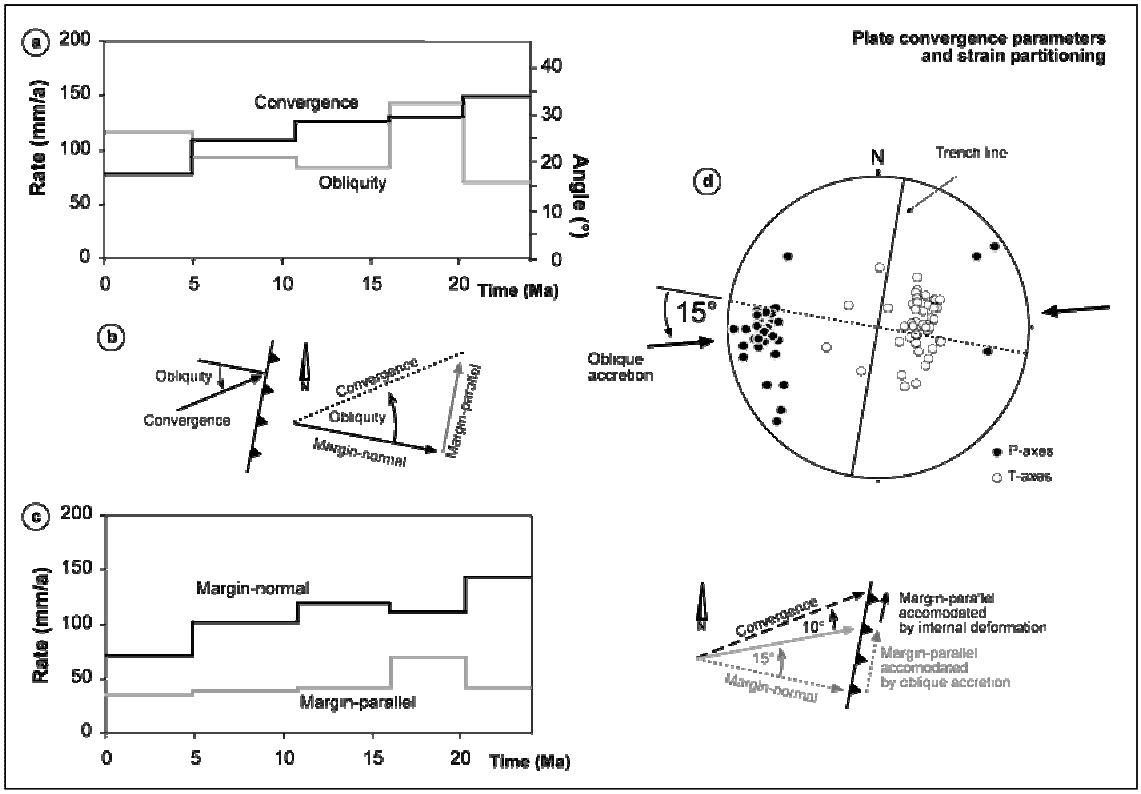

Fig. 7.6: *Plate kinematic constraints: (a) Nazca-South America plate convergence parameters during the Neogene (after Somoza, 1998), (b) decomposition of the plate convergence vector into margin-parallel and margin-normal components, (c) resulting components of margin-parallel and margin-normal shear, (d) P-axes of accretionary thrust earthquakes (Harvard CMT: offshore, 0-50 km depth, 1976-recent, 15-45°S; lower hemisphere, equal area plot) and strain partitioning between the plate interface and the overriding plate.*

7.6.2 Internal deformation of the fore-arc

Detached fore-arc blocks which move parallel to the margin due to oblique subduction (fore-arc slivers) are a common feature of active margins (Fitch, 1972, Jarrard, 1986, McCaffrey, 1992, Itoh et al., 2002, Sieh and Natawidjaja, 2000). In the Southern Andes, most authors agree that such a fore-arc sliver, the Chiloé block, exists north of the Chile Triple Junction (Lavenu and Cembrano, 1999, Beck, 1998, Nelson et al., 1994, Forsythe and Nelson, 1985). In contrast to active margins like Sumatra, where the sliver can move freely along the plate margin, however, the Chiloé block is supposed to be hindered in freely moving northward due to (1) the concave shape of the subduction zone (the Central Andean bend) and (2) flat-slab subduction between 28 and 32°S (Lavenu and Cembrano, 1999). This "buttress effect" (Beck, 1991, Beck et al., 1993) has been stressed by several authors to explain observed fore-arc deformation patterns. Garciá et al. (1988) and Rojas et al. (1994) attributed counterclockwise block rotations to such a buttress effect. Lavenu and Cembrano (1999) found field evidences for margin-parallel fore-arc shortening and interpreted these as manifestations of N-S compression due to the buttress effect. Potent (2003), based on field evidences for

coeval Pliocene to Quaternary margin-parallel fore-arc extension and shortening, suggest that the fore-arc periodically has been compressed and than reversely relaxed because oblique subduction pushes it northward against a buttress.

In contrast to these “compressional” buttress models, Vietor et al. (subm.) interpreted short term fore-arc extension obvious from GPS data (Klotz et al., 2001) as a consequence of differential Neogene backarc shortening in the Central Andes. They calculated that backarc shortening in the Central Andes may have theoretically made 71 - 116 km of space along the margin, which in their conceptual model is accommodated by margin-parallel fore-arc stretching and/or strike-slip movement along the LOFZ. The dextral displacement of 84 km (+66, -28) across the LOFZ, proposed by the kinematic model in this work, is almost identical to the space provided in the model of Vietor et al. (subm.) suggesting that most of the margin-parallel deformation induced by orocline formation probably has been localized along the LOFZ.